applied sciences

MDPI

Technical Note

Study of Cyclic Plasticity and Creep Ratchet Behavior of PTFE

Hongyan Liu, Lei Zhang, Kun Lu and Bingjun Gao *

School of Chemical Engineering and Technology, Hebei University of Technology, Tianjin 300130, China; 1995008@stu.hebut.edu.cn (H.L.); 202121502012@stu.hebut.edu.cn (L.Z.); lucky971115@163.com (K.L.)
* Correspondence: bjgao@hebut.edu.cn

Abstract: Due to its superior corrosion resistance and low coefficient of friction, polytetrafluoroethylene (PTFE) is extensively used in the aerospace, machinery, chemical, and pharmaceutical industries. However, PTFE components encounter complex alternating stresses, resulting in ratchet and creep, which will affect the component's reliability. It is therefore necessary to clarify the PTFE's resistance to ratchet and creep. In this paper, uniaxial ratchet and tensile creep experiments were conducted at five temperatures on a PTFE dog-bone tensile specimen. At various temperatures and stress levels, the effects of average stress and stress amplitude on the cyclic plastic behavior of PTFE were investigated. It is demonstrated that the ratchet strains and strain rates at 23 °C are greater than those at 50 °C. The reason for this is that the PTFE material exhibits different crystal states at these two temperatures. At temperatures above 50 °C, the ratchet strain and ratchet strain rate increase with temperature. At temperatures above 100 °C, the ratchet strain and ratchet strain rate of PTFE materials increase more rapidly due to the glass transition. By analyzing the creep strain and ratchet strain of specimens subjected to varying levels of average and amplitude stress, it was discovered that the creep strain and ratchet strain caused by the average stress under the same stress increment were greater than those caused by the amplitude stress.

Keywords: PTFE; cyclic plasticity; ratchet; tensile creep

check for updates

Citation: Liu, H.; Zhang, L.; Lu, K.; Gao, B. Study of Cyclic Plasticity and Creep Ratchet Behavior of PTFE. *Appl. Sci.* **2023**, *13*, 10039. https://doi.org/10.3390/app131810039

Academic Editor: Ilaria Cacciotti

Received: 15 August 2023
Revised: 30 August 2023
Accepted: 5 September 2023
Published: 6 September 2023

Copyright: © 2023 by the authors. Licensee MDPI, Basel, Switzerland. This article is an open access article distributed under the terms and conditions of the Creative Commons Attribution (CC BY) license (https://creativecommons.org/licenses/by/4.0/).

1. Introduction

Polytetrafluoroethylene (PTFE), which DuPont developed in 1938 [1], has since been widely applied in the aerospace, mechanical, chemical, and pharmaceutical industries due to its exceptional corrosion resistance and low coefficient of friction. At the same time, it exhibits excellent high- and low-temperature resistance, and can maintain good mechanical properties in the range of −196 to 260 °C [2].

In the materials and structures subjected to a cyclic stressing with non-zero mean stress, a cyclic accumulation of inelastic deformation will occur if the applied loading is high enough (ensuring that a yielding occurs), which is called ratcheting, or the ratcheting effect (some researchers have also called it "cyclic creep") [3]. The effects of average stress, stress amplitude, loading rate, loading path, and temperature on the ratchet behavior of metallic materials have been extensively investigated by researchers since the beginning of the 20th century [4–12]. Numerous researchers [13–22] have conducted a series of uniaxial and multiaxial ratchet tests on a large number of polymer materials—NBR (nitrile butadiene rubber), H-NBR (hydrogenated nitrile butadiene rubber), NR (natural rubber), PC (plastic), PEI (polyetherimide), PMMA (polymethyl methacrylate), UHMWPE (ultra-high-molecular-weight polyethylene), POM (polyoxymethylene), and ACFs (activated carbon fiber). The ratchet behavior of polymers is, to a certain extent, dependent on the polymer's molecular structure. The response to the average and amplitude stresses is comparable for different polymers. For example, they are all similar, with ratcheting being more pronounced at higher stress levels.

When PTFE is used in gaskets under preload and alternating pressure load [23], creep and ratchet would often occur. Chen and Hui [24] and Zhang et al. [25] studied the ratch-

eting behavior of PTFE under cyclic compression, and Zhang et al. [23] and Zhang and Chen [26] studied the ratcheting behavior of PTFE at room temperature and high temperature. Zheng et al. [27,28] examined the ratcheting behavior of PTFE gaskets under cyclic compressive loading, with small stress amplitude, and creep ratchet deformation under compressive creep-fatigue loading, with small stress amplitude at various temperatures. However, PTFE membranes and PTFE-lined tubes are also subjected to tensile stresses in service, and little is known about the relationship between PTFE's tensile creep and ratcheting effects at various temperatures.

In this study, PTFE dog-bone tensile specimen were experimentally studied by applying constant tension and cyclic uniaxial loading at temperatures ranging from 23 to 200 °C. The ratchet and creep behaviors of PTFE at different temperatures were investigated.

2. Experiments

The PTFE raw material used in this experiment was provided by Zhejiang Juhua Company in Zhejiang Province, China. According to the Chinese standard GB/T11546.1-2008 [29], the cylindrical bar produced by extrusion molding is transformed into a dog-bone tensile specimen, which is illustrated in Figure 1.

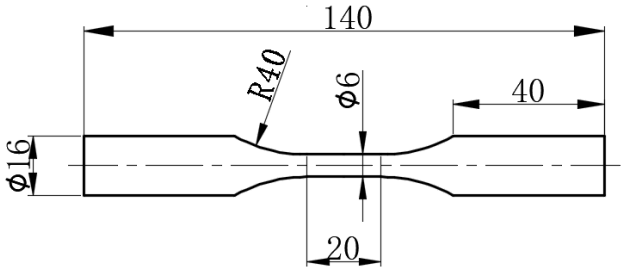


Figure 1. Specimen geometry (mm).

The test device is an electronic servo loading system EUM-25K20 produced by CARE Measurement and Control Company of China, and the heating chamber is a small ceramic electric heating box designed by Tianjin University. The experimental setup is shown in Figure 2.

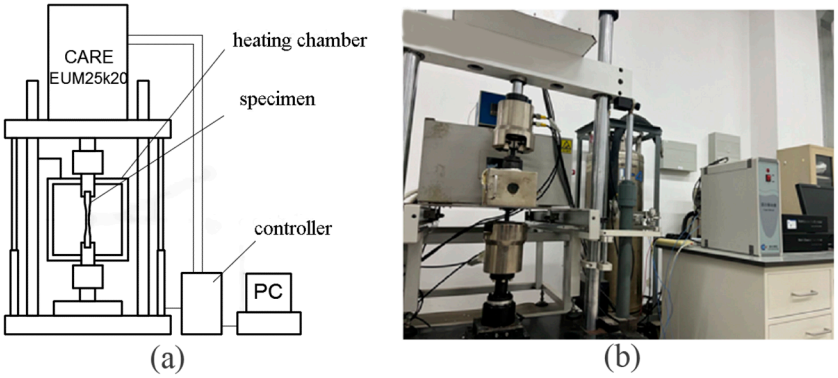


Figure 2. Testing rig (**a**) sketch; (**b**) setup.

In order to ensure the uniformity of the specimen's temperature distribution, the clamped specimen is heated to the test temperature and held at this temperature for 30 min before the pertinent test is conducted. According to the international standard ISO 527-1-2012 [30], the tensile deformation rate in uniaxial tensile tests is 0.25 mm/min. The cyclic plasticity test protocol was designed in accordance with the yield limit of PTFE at various temperatures, as detailed in Table 1, where $\sigma^T{}_s$ is the nominal yield strength at the corresponding temperature, and LC1(Load Case 1)-LC5 represent different working conditions. According to Zhang's experimental results [26], it can be seen that the effect

is no longer particularly significant when the loading rate is greater than about 10 N/s. Combined with the practical application of PTFE-lined pipe, the loading rate of the ratchet test is 18 N/s. To ensure that the ratchet strain can reach the expected state of ratchet development, the number of cyclic loadings is set to 200 for all temperatures.

Table 1. Cyclic plasticity experiments scheme.

$S_m/\sigma^T{}_S$ \ $S_a/\sigma^T{}_S$	**0.5**	**0.6**	**0.7**
0.6		LC1	
0.7	LC2	LC3	LC4
0.8		LC5	

At 23 °C, 50 °C, 100 °C, 150 °C, and 200 °C, PTFE specimens were subjected to tensile creep experiments with creep stresses of $S = 1.7\sigma^T{}_s$, $1.5\sigma^T{}_s$, $1.3\sigma^T{}_s$, $1.1\sigma^T{}_s$, and $0.9\sigma^T{}_s$, respectively. These creep tests encompass the range of stress changes observed in the cyclic plasticity tests conducted at five temperatures.

The ratchet strain is defined in Equation (1).

$$\varepsilon_r = \frac{1}{2}(\varepsilon_{\max} + \varepsilon_{\min}), \tag{1}$$

where ε_{max} and ε_{min} represent the maximum and minimum strain values per cycle revolution, respectively. Since all the stresses/strains obtained in the experiments are engineering stresses σ/strains ε, their magnitudes are related to the real stresses σ_T/strains ε_T as: $\sigma_T = \sigma\ln(1+\varepsilon)$; $\varepsilon_T = \ln(1+\varepsilon)$, respectively.

The ratchet strain rate is defined in Equation (2) [26,31].

$$\dot{\varepsilon_r} = \frac{d\varepsilon_r}{dN}, \tag{2}$$

where N is the number of cycles.

3. Results and Discussion

3.1. Uniaxial Tensile Tests at Different Temperatures

Figure 3 depicts the uniaxial tensile curves at five temperatures. The modulus of elasticity was obtained by fitting a straight line to the initial linear part of the stress–strain curve using the least squares method. Since PTFE does not have a readily apparent yield point, the stress value of 0.2% residual deformation is used to define its nominal yield stress, as shown in Table 2. The modulus of elasticity and the nominal yield stress of PTFE, as well as the material's tensile strength, decrease considerably as the temperature rises, as shown in Figure 3. However, this decrease is not completely linear. This may be due to the fact that the crystal structure of the PTFE material changes as the temperature increases.

Table 2. The elastic modulus and nominal yield limit of PTFE at different temperatures.

Temperature/°C	**Elastic Modulus/MPa**	**Nominal Yield Limit/MPa**
23	317	5.3
50	182	3.2
100	108	1.8
150	40	1.3
200	22	1

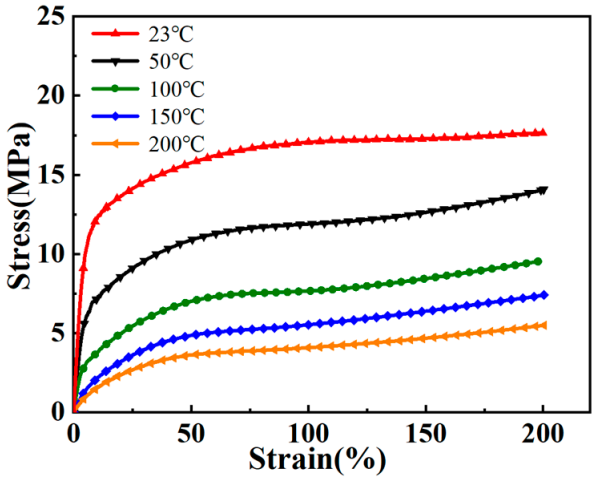


Figure 3. The uniaxial tensile curves of PTFE at different temperatures.

3.2. The Cyclic Plasticity Behavior at Different Temperatures

The cyclic plasticity test was performed on PTFE specimens at different temperatures with different average stresses and amplitude stresses. The cyclic plasticity hysteresis curves are only given for the 23 °C condition as examples, which shown in Figure 4. Ratchet strains apparently appeared in each loading condition, and the area of the hysteresis loop gradually decreased with the increase in the number of cycles. This indicates that the material shows a more pronounced hardening when plastic deformation occurs.

Figure 5 illustrates the variation in ratchet strain and strain rate for each loading condition. It reveals that the ratchet strain increases gradually with the number of cycles, but the ratchet strain rate decreases rapidly. Among the cycles, it accumulates rapidly in the first 20 cycles and gradually increases at a relatively stable rate after 20 cycles. Under different average stresses, the material initial single tensile rise section curve change trend is basically the same, indicating that PTFE in uniaxial ratchet test conditions under the stability of the stress–strain response and the rapid accumulation of ratcheting strain still occurs in the first 20 cycles. After 50 cycles, the evolution of the ratchet strain rate during loading is more or less the same, and the ratchet strain and ratchet strain rate are very sensitive to the stress response. At the same average stress, the ratchet strain and strain rate increased gradually with the increase in amplitude stress. However, at different average stresses, with the increase in average stress at the same amplitude stress, the increment of ratchet strain after 200 cycles changed significantly, a larger level of increase was observed relative to the different amplitude stresses, and the change in the ratchet strain rate was more prominent. Notably, the ratchet strain and the strain rate at 23 °C are greater than those at 50 °C. This is because PTFE exhibits three different crystalline phases at atmospheric pressure. The three polymorphs are usually denoted as form II, stable at temperatures below 19 °C, form IV, stable at temperatures between 19 and 30 °C, and form I, stable at temperatures higher than 30 °C up to the melting point of 330 °C [32]. Furthermore, by looking at the electron diffraction patterns of form IV and form I, it was found that the structures of the two forms are indeed different [33]. The present experimental data illustrate that the ratchet strain and ratchet strain rate of crystalline type IV at 23 °C are larger than those of crystalline type I at 50 °C.

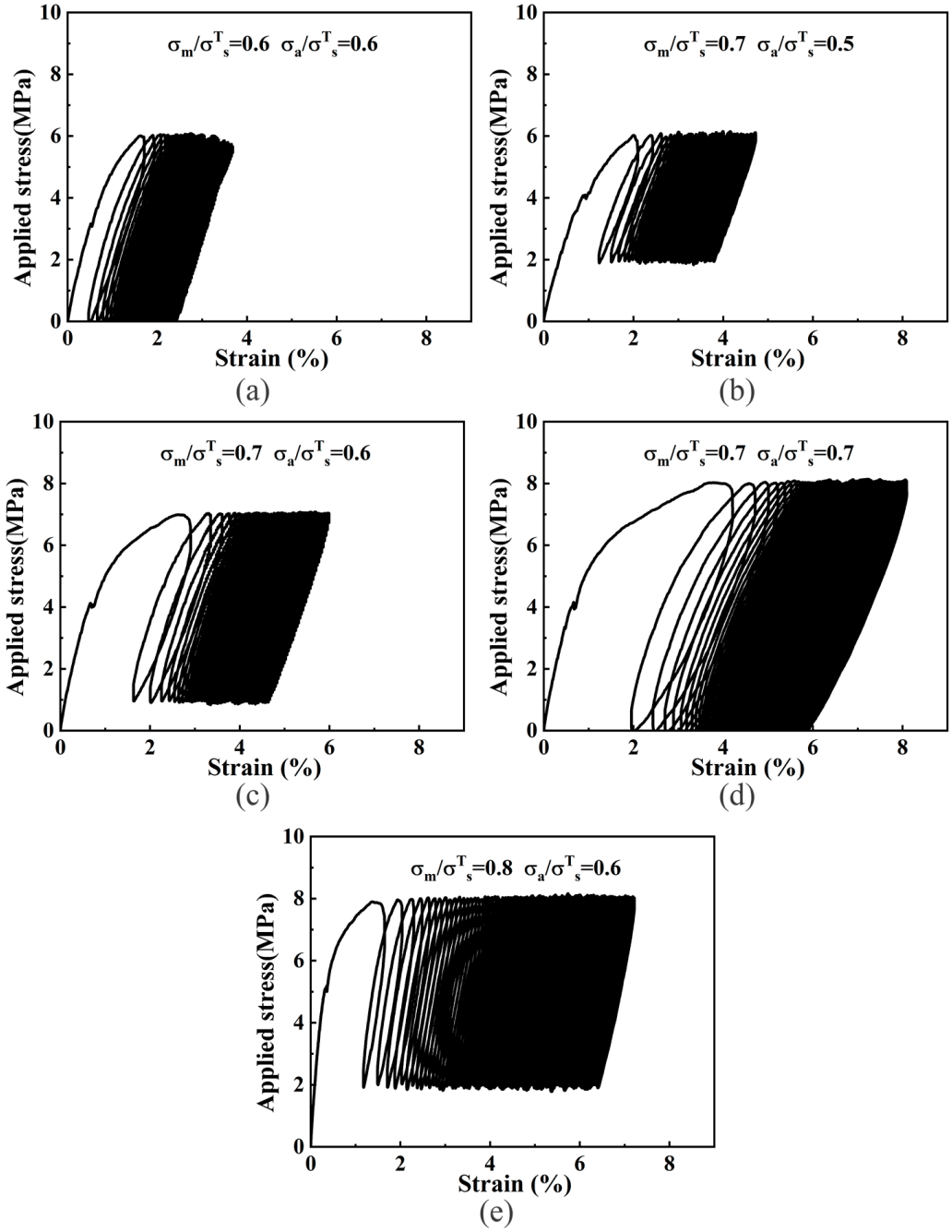


Figure 4. The cyclic hysteresis curves under different stress amplitudes at 23 °C: (**a**) LC1; (**b**) LC2; (**c**) LC3; (**d**) LC4; (**e**) LC5.

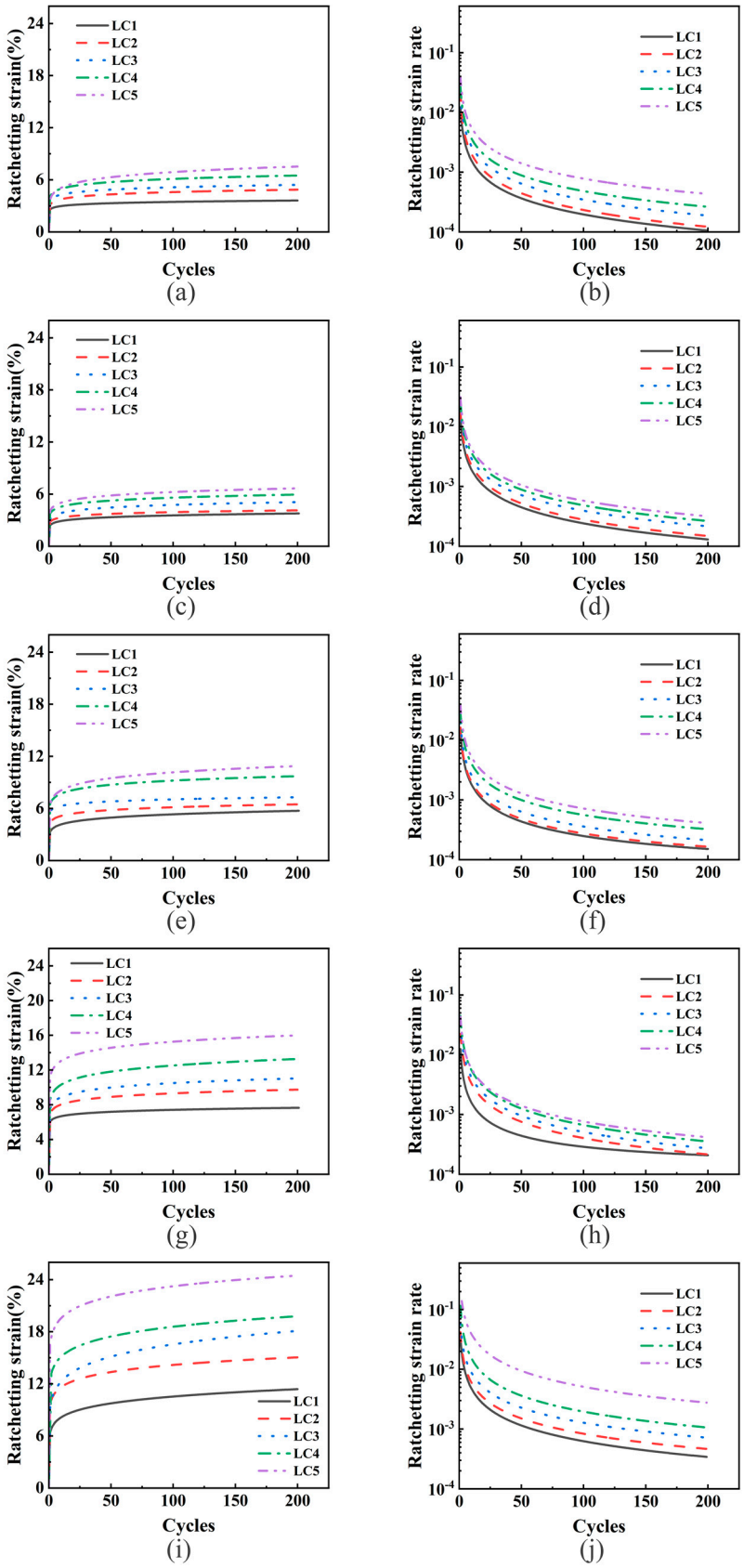


Figure 5. Ratchet strain and strain rate under different loading conditions Ratchet strain: (**a**) 23 °C; (**c**) 50 °C; (**e**) 100 °C; (**g**) 150 °C; (**i**) 200 °C. Ratchet strain rate: (**b**) 23 °C; (**d**) 50 °C; (**f**) 100 °C; (**h**) 150 °C; (**j**) 200 °C.

Moreover, throughout the temperature data, for both the ratchet strain and strain rate, LC3 is in the middle, with LC2 below and LC4 above, which indicates that for the same level of average stress, both the ratchet strain and ratchet strain rate increase with the increase in amplitude stress level. Similarly, LC3 is in the middle, with LC1 below and LC5 above, which indicates that for a given level of amplitude stress, the ratchet strain and ratchet strain rate increase as the average stress level rises. Furthermore, LC1 is lower than LC2, and LC5 is higher than LC4, which indicates that an equal increase in the average stress level has a greater effect on ratchet strain and strain rate than an equal increase in the stress magnitude level. One possible explanation is that the average stress tends to be associated with creep. Higher average stresses result in larger creep responses.

In the load ranges discussed, the effect of changes in mean stress on ratchet strain is more pronounced than that of changes in amplitude stress, and the effect on ratchet strain rate is similar to that of ratchet strain, whether the load is increased or decreased. The difference between the effects of mean stress and magnitude stress on ratchet strain is progressively magnified as the temperature increases. When cyclic loading is returned to no load at five temperatures, there is almost no difference in deformation between LC1 and LC2; LC4 and LC5, and the difference between mean stress and amplitude stress has little effect on the recoverable deformation due to simple molecular units.

The results of LC3 at different temperatures not less than 50 °C are depicted in Figure 6. After 200 cycles, the ratchet strain reaches 5.44%, 5.62%, 6.8%, 11.2%, and 18.5%, respectively, which shows that the PTFE ratchet behavior is very sensitive to the temperature response, and the ratchet deformation is progressively larger as the temperature increases with the loading of the load at the same stress level; there is no significant difference in the ratchet behavior before 100 °C, and after 100 °C, the ratchet strain increases significantly. The evolution of the ratchet strain rate is close to that expected according to the rule, i.e., in the first cycle up to 50 cycles, the rate is rapidly reduced, and then maintains a relatively stable rate of slow decline. In general, below 150 °C, the ratchet strain rate difference is not significant, but when the temperature reaches 200 °C, the ratchet strain rate will exhibit nearly three times the increase. PTFE special high-temperature characteristics force us to consider the impact of the cyclic plastic loading process caused by the creep behavior, which may occur due to the influence of the cyclic plastic loading process. This may be an important factor affecting the cyclic plasticity test results. Both the ratchet strain and the strain rate increase with increasing temperatures. However, as shown in Figure 6b, the rate of ratchet strain increase rises significantly above 100 °C. This is because PTFE's modulus of elasticity decreases significantly once the ambient temperature surpasses 100 °C. The increase in temperature alters the structure of the crystal arrangement, and according to Gérard et al., this material undergoes a glassy transition at around 130 °C [34]. Meanwhile, the amorphous organization between the PTFE crystals and the crystals of other materials is progressively parallel to the slip in the crystal region; the higher the temperature, the greater the degree of slip [32]. As slippage occurs, the tendency of crystals to deform in the axial direction of tensile stress through rotation becomes more pronounced.

The maximum creep strain at 23 °C is 2.3, 3.1, 5.9, and 7.8 times the minimum creep strain, respectively, which can be seen to increase substantially with the increasing stress level. The maximum creep strain at 50 °C was 1.34, 1.92, 2.68, and 3.58 times the minimum creep strain, respectively. The values at 100 °C were 1.38, 1.86, 2.75, and 3.68. The values at 150 °C were 1.46, 2.07, 3.15, and 4.32. The values were 1.5, 2.25, 3.13, and 4.25 at 200 °C. It can be seen that at 50 to 100 °C, the different levels of creep strain were similar. The stress response to temperatures between 150 and 200 °C is more sensitive, and the rule of change is similar.

3.3. Static Creep Tests and Determination of Creep Equations

3.3.1. Static Creep at Different Temperatures

The results of tensile creep experiments conducted on PTFE specimens at 23 °C, 50 °C, 100 °C, 150 °C, and 200 °C, with creep stresses of $S/\sigma^T{}_s$ = (1.7, 1.5, 1.3, 1.1, 0.9), are

depicted in Figure 7. Although the evolution of tensile creep over time can be divided into three stages, namely the decelerated creep stage, the stable development stage, and the accelerated creep stage; the 25 groups of tests in Figure 7 did not reach the stage of accelerated creep and rupture due to the limitations of the test time. In the initial stage of the test, the creep rate of PTFE decreased rapidly, and then in the stable stage, the creep rate remained constant within the test duration.

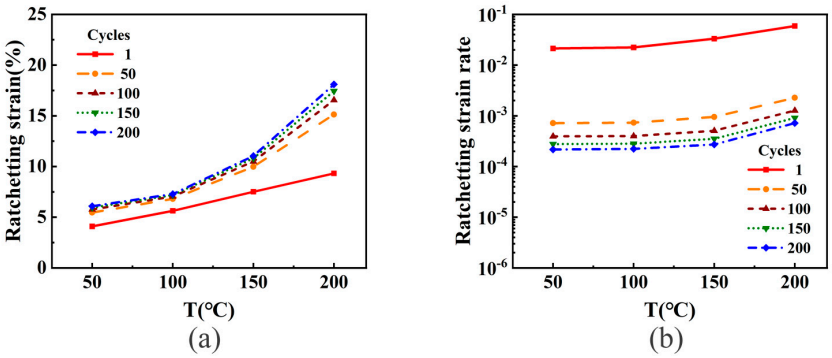


Figure 6. Comparison of results of cyclic plasticity tests at different temperatures: (**a**) ratchet strain; (**b**) ratchet strain rate.

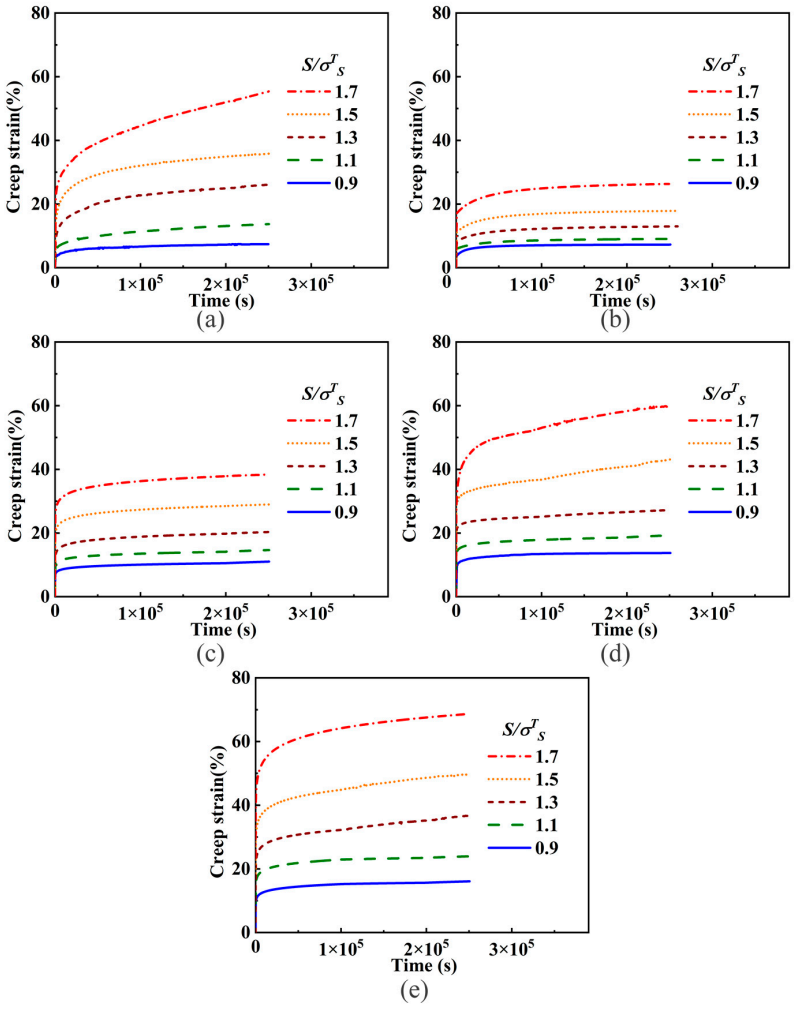


Figure 7. Creep deformation of PTFE at different temperatures: (**a**) 23 °C; (**b**) 50 °C; (**c**) 100 °C; (**d**) 150 °C; (**e**) 200 °C.

Figure 7 demonstrates that, at the same temperature, the creep deformation is proportional to the creep stress level. However, creep behaves differently with different temperature ranges. In the range of 50 to 200 °C, with the increase in temperature, it would exhibit more creep deformation for the same creep stress. This is because the free volume of the material and molecular thermal momentum will increase with temperature, and the relaxation time for relative movement will be reduced [35]. However, in the range of 23–50 °C, the present experimental data illustrate that the creep strain and creep strain rate of crystalline type IV at 23 °C is greater than that of crystalline type I at 50 °C [32,33].

3.3.2. Determination of the Creep Equation

Considering only the steady state creep stage, the Arrhenius equation [36,37] describes the creep rate in Equation (3).

$$\dot{\varepsilon} = A\sigma^n \exp(-\frac{Q_a}{RT}), \tag{3}$$

where $\dot{\varepsilon}$ is the steady state creep rate, A is a material constant, σ is the creep stress, Q_a is the nominal creep activation energy, n is the stress index [38,39], R is the gas constant, and T is the absolute temperature. As shown in Figure 8a, the steady creep rate is derived from the stable stage of the creep curve at various temperatures and stress levels.

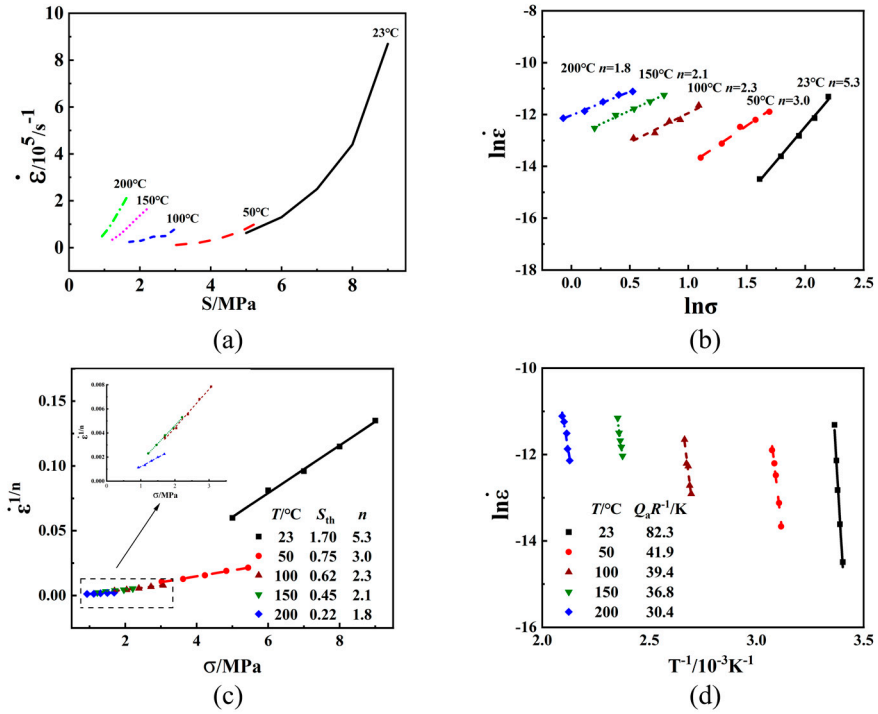


Figure 8. Creep parameters at various temperatures: (**a**) steady state creep rate; (**b**) stress index; (**c**) creep stress threshold value; (**d**) creep activation energy.

The stress index n and the creep activation energy Q_a of the creep steady state phase are determined according to Equations (4) and (5), respectively.

$$n = \frac{\partial \ln \dot{\varepsilon}}{\partial \ln \sigma}. \tag{4}$$

$$Q_a = -R(\frac{\partial \ln \dot{\varepsilon}}{\partial T^{-1}}). \tag{5}$$

Due to the material's inherent resistance to deformation, it is believed that the propelling force for creep deformation is not the applied stress, but rather the effective stress S- S_{th}, where S_{th} is the creep stress threshold. In this paper, the trial algorithm is used to solve the stress index and creep threshold. Firstly, S_{th} is assumed to be equal to 0. Then the $ln\dot{\varepsilon} \sim ln\sigma$ curve is plotted based on the experimental data, and the slope of the fitted curve in the figure is the initial n value. After plotting the $\dot{\varepsilon}^{\frac{1}{n}} \sim \sigma$ curve and extrapolating the fitted curve to $\dot{\varepsilon}^{\frac{1}{n}} = 0$, the creep threshold stress value S_{th} can be obtained. According to this method, repeated trial calculations can finally obtain the stress index and creep stress threshold at different temperatures. The creep parameters at each temperature are shown in Table 3.

Table 3. Creep parameters at each temperature.

T/°C	n	S_{th}/MPa	A	Q_aR^{-1}/K
23	5.3	1.70	1.32×10^{-9}	82.3
50	3.0	0.75	6.18×10^{-8}	41.9
100	2.3	0.62	5.52×10^{-7}	39.4
150	2.1	0.45	7.11×10^{-7}	36.8
200	1.8	0.22	5.48×10^{-6}	30.4

From the experimental data, it can be seen that the creep stress index n (Figure 8b) and creep stress threshold value Q_a (Figure 8c) decrease with the increase in temperature, which can be divided into two stages of change. At 23 to 50 °C, n and Q_a decrease rapidly, while at 50 to 200 °C, n and Q_a decrease at a relatively low rate.

3.4. Extraction of Creep Strain from Ratchet Strain

Assuming that S_{max} and S_{min}, respectively, are the maximum and minimum stresses of the triangular wave pulsing cyclic loading of the test, the stress variation for each cyclic loading is shown in Equations (6) and (7).

$$S(t) = S_{min} + \frac{2t}{T}(S_{max} - S_{min}), t \in [0, \frac{T}{2}]. \quad (6)$$

$$S(t) = S_{max} + (1 - \frac{2t}{T})(S_{max} - S_{min}), t \in [\frac{T}{2}, T]. \quad (7)$$

The upper and lower limits of the integration time correspond to the time of maximum stress and the creep stress threshold in cyclic plasticity, respectively. The cyclic creep strain generated by each cyclic loading can then be expressed as Equation (8).

$$\begin{aligned} \varepsilon = A\int_{t_0}^{\frac{T}{2}}[S_{min} + \tfrac{2t}{T}(S_{max} - S_{min}) - S_{th}]^n \exp(-Q_a/RT)dt \\ + A\int_{\frac{T}{2}}^{T-t_0}[S_{max} + (1 - \tfrac{2t}{T})(S_{max} - S_{min}) - S_{th}]^n \exp(-Q_a/RT)dt \end{aligned} \quad (8)$$

where t_0 is the time corresponding to S_{th}, when the loaded minimum stress value $S_{min} \geq S_{th}$, $t_0 = 0$. Substituting the creep equations for different temperatures into the above equation yields the value of creep in the cyclic loading at each temperature and each stress level, as shown in Table 4.

Table 4. Creep strain at each temperature for 200 cycles.

Condition	23 °C	50 °C	100 °C	150 °C	200 °C
LC1	0.34%	0.18%	0.35%	0.58%	0.86%
LC2	0.42%	0.23%	0.46%	0.65%	1.07%
LC3	0.43%	0.25%	0.48%	0.71%	1.12%
LC4	0.44%	0.26%	0.50%	0.76%	1.15%
LC5	0.48%	0.32%	0.59%	0.92%	1.23%

At various temperatures and cyclic stress levels, the maximum percentage of creep strain in the total strain for 200 cycles of loading does not exceed 7%. At the same creep stress level, the percentage of creep strain in the total cyclic plastic strain at 23 °C remains greater than that at 50 °C, which is related to the different types of crystalline phases of PTFE below and above 30 °C. The percentage of creep strain begins to rise with the temperature when it reaches 100 °C. Evidently, the creep deformation is more sensitive to average stress change.

3.5. Ratchet Strain after Creep Removal

The results of cyclic plasticity presented in Section 3.2 indicate that the difference between the average stress change and the ratchet strain and ratchet strain rate is more pronounced than the amplitude stress. After removing the creep strain from the cyclic plasticity results, it can be seen that the difference in ratchet strain caused by the average stress is still more significant than the amplitude stress. Several researchers have studied the ratchet effect in the past, and by analyzing the work of Li (Zr-4 zirconium alloy), Yin (PE100 polyethylene), and Yu (natural rubber) [40–42], it was determined that the difference in ratchet strains and the ratchet strain rate due to the change in the average stress was more pronounced. However, Li (S30408 metastable austenitic stainless steel), Jiang (304 austenitic stainless steel), and Peng (6005 aluminum alloy) [43–45] demonstrated that the variation in ratchet strain and ratchet strain rate due to amplitude stress variation was more pronounced. This phenomenon is inferred to be related to the material's own specific properties.

4. Conclusions

In this paper, the uniaxial ratchet and tensile creep behavior of a PTFE dog-bone tensile specimen at various temperatures and stress levels were investigated and discussed systematically, and the following conclusions were drawn.

1. The ratchet strain and strain rate at 23 °C were greater than those at 50 °C, and the ratchet strain and ratchet strain rate increase with an increase in temperature when the temperature exceeds 50 °C. When the temperature exceeds 100 °C, the rate of increase rises.
2. The stable creep strain and strain rate at 23 °C were greater than those at 50 °C. The stabilized creep strain and the creep strain rate increase with increasing temperature when the temperature exceeds 50 °C. The rate of increase was faster when the temperature exceeded 100 °C.
3. The ratchet strain and ratchet strain rate, creep strain, and creep strain rate at 23 °C were higher than those at 50 °C because PTFE has a different crystalline shape at 23 °C and 50 °C. Above 100 °C, the more rapid increase may be due to the glassy transition of the PTFE material at about 130 °C.
4. For PTFE under uniaxial cyclic loading, the ratchet strain and strain rate, as well as the creep strain and steady creep strain rate, were more sensitive to average stress change.

Author Contributions: Experiments: K.L. and L.Z.; data curation: L.Z. and K.L.; methodology: K.L. and H.L.; conceptualization: B.G. and H.L.; writing—original draft preparation: L.Z.; writing—review and editing: B.G., H.L. and L.Z.; project administration: B.G.; funding acquisition: B.G. All authors have read and agreed to the published version of the manuscript.

Funding: This research was supported by the National Key Research and Development Program of China, No.2018YFC0808600.

Conflicts of Interest: The authors declare no conflict of interest.

References

1. Bergström, J.S.; Hilbert, L.B. A constitutive model for predicting the large deformation thermomechanical behavior of fluoropolymers. *Mech. Mater.* **2005**, *37*, 899–913. [CrossRef]
2. Cui, S. Polytetrafluoroethylene fiber with excellent resistance. *Text. Sci. Res.* **2019**, *9*, 54–59.
3. Kang, G. Ratchetting: Recent progresses in phenomenon observation, constitutive modeling and application. *Int. J. Fatigue* **2008**, *30*, 1448–1472. [CrossRef]
4. Kang, G.; Gao, Q.; Yang, X. Uniaxial and non-proportionally multiaxial ratcheting of SS304 stainless steel at room temperature: Experiments and simulations. *Int. J. Non-Linear Mech.* **2004**, *39*, 843–857. [CrossRef]
5. Wu, D.; Xuan, F.; Guo, S.; Zhao, P. Uniaxial mean stress relaxation of 9–12% Cr steel at high temperature: Experiments and viscoplastic constitutive modeling. *Int. J. Plast.* **2016**, *77*, 156–173. [CrossRef]
6. Chen, X.; Jiao, R.; Kim, K.S. On the Ohno–Wang kinematic hardening rules for multiaxial ratcheting modeling of medium carbon steel. *Int. J. Plast.* **2005**, *21*, 161–184. [CrossRef]
7. Chen, X.; Jiao, R. Modified kinematic hardening rule for multiaxial ratcheting prediction. *Int. J. Plast.* **2004**, *20*, 871–898.
8. Yaguchi, M.; Takahashi, Y. Ratchetting of viscoplastic material with cyclic softening, part 1: Experiments on modified 9Cr–1Mo steel. *Int. J. Plast.* **2005**, *21*, 43–65. [CrossRef]
9. Chen, X.; Yu, D.-H.; Kim, K.S. Experimental study on ratcheting behavior of eutectic tin–lead solder under multiaxial loading. *Mater. Sci. Eng. A* **2005**, *406*, 86–94. [CrossRef]
10. Hassan, T.; Kyriakides, S. Ratcheting in cyclic plasticity, part I: Uniaxial behavior. *Int. J. Plast.* **1992**, *8*, 91–116. [CrossRef]
11. Kang, G.; Li, Y.; Zhang, J.; Sun, Y.; Gao, Q. Uniaxial ratcheting and failure behaviors of two steels. *Theor. Appl. Fract. Mech.* **2005**, *43*, 199–209. [CrossRef]
12. Ohno, N.; Wang, J.D. Kinematic hardening rules with critical state of dynamic recovery, part I: Formulation and basic features for ratchetting behavior. *Int. J. Plast.* **1993**, *9*, 375–390. [CrossRef]
13. Ma, J.; Gao, H.; Gao, L.; Chen, X. Uniaxial ratcheting behavior of anisotropic conductive adhesive film at elevated temperature. *Polym. Test.* **2011**, *30*, 571–577. [CrossRef]
14. Shariati, M.; Hatami, H.; Yarahmadi, H.; Eipakchi, H.R. An experimental study on the ratcheting and fatigue behavior of polyacetal under uniaxial cyclic loading. *Mater. Des.* **2012**, *34*, 302–312. [CrossRef]
15. Chen, K.; Kang, G.; Lu, F.; Xu, J.; Jiang, H. Temperature-dependent uniaxial ratchetting of ultra-high molecular weight polyethylene. *Fatigue Fract. Eng. Mater. Struct.* **2016**, *39*, 839–849. [CrossRef]
16. Liu, W.; Gao, Z.; Yue, Z. Steady ratcheting strains accumulation in varying temperature fatigue tests of PMMA. *Mater. Sci. Eng. A* **2008**, *492*, 102–109. [CrossRef]
17. Pan, D.; Kang, G.; Zhu, Z.; Liu, Y. Experimental study on uniaxial time-dependent ratcheting of a polyetherimide polymer. *J. Zhejiang Univ.-Sci. A* **2010**, *11*, 804–810. [CrossRef]
18. Yu, W.; Chen, X.; Wang, Y.; Yan, L.; Bai, N. Uniaxial ratchetting behavior of vulcanized natural rubber. *Polym. Eng. Sci.* **2008**, *48*, 191–197. [CrossRef]
19. Jiang, H.; Zhang, J.; Kang, G.; Xi, C.; Jiang, C.; Liu, Y. A test procedure for separating viscous recovery and accumulated unrecoverable deformation of polymer under cyclic loading. *Polym. Test.* **2013**, *32*, 1445–1451. [CrossRef]
20. Lu, F.; Kang, G.; Jiang, H.; Zhang, J.; Liu, Y. Experimental studies on the uniaxial ratchetting of polycarbonate polymer at different temperatures. *Polym. Test.* **2014**, *39*, 92–100. [CrossRef]
21. Chen, Y.; Kang, G.; Tao, R.; Jiang, H. Experimental Studies on Deformation Behaviors of Rubbery Materials under Cyclic Loading. *Appl. Mech. Mater.* **2017**, *853*, 106–111. [CrossRef]
22. Wang, Y.; Yu, W.; Yan, L.; Chen, X. Ratchetting behaviour of nitrile butadiene rubber material. *Plast. Rubber Compos.* **2007**, *36*, 134–140. [CrossRef]
23. Zhang, Z.; Chen, X.; Wang, Y. Uniaxial ratcheting behavior of polytetrafluoroethylene at elevated temperature. *Polym. Test.* **2010**, *29*, 352–357. [CrossRef]
24. Chen, X.; Hui, S. Ratcheting behavior of PTFE under cyclic compression. *Polym. Test.* **2005**, *24*, 829–833. [CrossRef]
25. Zhang, Z.; Chen, X.; Wang, T. A simple constitutive model for cyclic compressive ratchetting deformation of polyteterafluoroethylene (PTFE) with stress rate effects. *Polym. Eng. Sci.* **2008**, *48*, 29–36. [CrossRef]
26. Zhang, Z.; Chen, X. Multiaxial ratcheting behavior of PTFE at room temperature. *Polym. Test.* **2009**, *28*, 288–295. [CrossRef]
27. Zheng, X.; Wen, X.; Wang, W.; Gao, J.; Lin, W.; Ma, L.; Yu, J. Creep-ratcheting behavior of PTFE gaskets under various temperatures. *Polym. Test.* **2017**, *60*, 229–235. [CrossRef]

28. Zheng, X.; Wen, X.; Gao, J.; Lin, W.; Ma, L.; Yu, J. Temperature-dependent ratcheting of PTFE gaskets under cyclic compressive loads with small stress amplitude. *Polym. Test.* **2017**, *57*, 296–301. [CrossRef]
29. *GB/T11546.1-2008*; Plastic-Determination of Creep Behavior-Part 1: Tensile Creep. China Standard Publishing House: Beijing, China, 2016.
30. *ISO527-1-2012*; Plastics—Determination of Tensile Properties-Part 1: General Principles. International Standard Publishing House: Geneva, Switzerland, 2012.
31. McDowell, D.L. Stress state dependence of cyclic ratchetting behavior of two rail steels. *Int. J. Plast.* **1995**, *11*, 397–421. [CrossRef]
32. Sperati, C.A.; Starkweather, H.W. *Fluorine-Containing Polymers. II. Polytetrafluoroethylene*; Springer: Berlin/Heidelberg, Germany, 1961. [CrossRef]
33. Clark, E.S. The Crystal Structure of Polytetrafluoroethylene, Forms I and IV. *J. Macromol. Sci. Part B Phys.* **2006**, *45*, 201–213. [CrossRef]
34. Calleja, G.; Jourdan, A.; Ameduri, B.; Habas, J.-P. Where is the glass transition temperature of poly(tetrafluoroethylene)? A new approach by dynamic rheometry and mechanical tests. *Eur. Polym. J.* **2013**, *49*, 2214–2222. [CrossRef]
35. D'Amore, M.; Talarico, G.; Barone, V. Periodic and High-Temperature Disordered Conformations of Polytetrafluoroethylene Chains: An ab Initio Modeling. *J. Am. Chem. Soc.* **2006**, *128*, 1099–1108. [CrossRef] [PubMed]
36. Purushothaman, S.; Tien, J.K. Role of back stress in the creep behavior of particle strengthened alloys. *Acta Met.* **1978**, *26*, 519–528. [CrossRef]
37. Mukherjee, A.K. An examination of the constitutive equation for elevated temperature plasticity. *Mater. Sci. Eng. A* **2002**, *322*, 1–22. [CrossRef]
38. Barboza, M.J.R.; Perez, E.A.C.; Medeiros, M.M.; Reis, D.A.P.; Nono, M.C.A.; Neto, F.P.; Silva, C.R.M. Creep behavior of Ti–6Al–4V and a comparison with titanium matrix composites. *Mater. Sci. Eng. A* **2006**, *428*, 319–326. [CrossRef]
39. Evans, W.J.; Harrison, G.F. Power law steady state creep in α/β titanium alloys. *J. Mater. Sci.* **1983**, *18*, 3449–3455. [CrossRef]
40. Li, H. Study of Anisotropic Uniaxial Ratchet Behavior of Zr-4 Alloy. Master's Thesis, Tianjin University, Tianjin, China, 2013.
41. Yin, J. Experimental Study of Cyclic Plasticity of PE100 Pipe. Master's Thesis, Hebei University of Technology, Tianjin, China, 2014.
42. Yu, W. Multiaxial Fatigue Life Study of Rubber Materials. Master's Thesis, Tianjin University, Tianjin, China, 2007.
43. Li, L. Study of the Low-Temperature Ratchet Effect of Pre-Strained S30408. Master's Thesis, Hebei University of Technology, Tianjin, China, 2019.
44. Jiang, G. Study of Ratchet Stabilization Effect on Pressure Vessel of 304 Austenitic Stainless Steel. Ph.D. Thesis, East China University of Science and Technology, Shanghai, China, 2014.
45. Peng, J. A Study of Ratcheting and Low-Week Fatigue Behavior of Aluminum Alloys. Master's Thesis, Southwest Jiaotong University, Chengdu, China, 2014.

Disclaimer/Publisher's Note: The statements, opinions and data contained in all publications are solely those of the individual author(s) and contributor(s) and not of MDPI and/or the editor(s). MDPI and/or the editor(s) disclaim responsibility for any injury to people or property resulting from any ideas, methods, instructions or products referred to in the content.